European Conference on Computational Fluid Dynamics
ECCOMAS CFD 2006
P. Wesseling, E. Oñate and J. Périaux (Eds)

NUMERICAL SCHEMES FOR THE SIMULATION OF THREE-DIMENSIONAL CARDIAC ELECTRICAL PROPAGATION IN PATIENT-SPECIFIC VENTRICULAR GEOMETRIES

A.M. Rosolen[1], S. Ordas[1], M. Vázquez[2,3] and A.F. Frangi[1]

[1]Pompeu Fabra University, Department of Technology, CILab
Campus Francia, 08003 Barcelona, Spain
e-mail: {adrian.rosolen, sebastian.ordas, alejandro.frangi}@upf.edu

[2]Barcelona Supercomputing Center, UPC
Nexus II - Campus Nord, 08034 Barcelona, Spain

[3] Universitat de Girona, GREFEMA
Campus de Montilivi, 17071 Girona, Spain
e-mail: mariano.vazquez@udg.es

Key words: Computational Electrophysiology, Finite Element Method, Bidomain Model, FitzHugh Nagumo Equations, Shock Capturing Techniques.

Abstract. *This paper introduces different numerical strategies in computational electrophysiology, based on the Finite Element Method to handle the space discretization of the governing equations. The long-term goal is to apply these computational techniques to study the three-dimensional electrical propagation in patient-specific ventricular geometries, having in mind not only to understand the process, but also to use the simulation tools to improve the diagnosis accuracy.*

The electrical response of cardiac tissue is modeled by combining Bidomain (BD) and FitzHugh-Nagumo (FHN) models. The BD model uses two coupled diffusion PDEs to handle the electrical potential in the intra- and extracellular domains of cardiac tissue taking into account the anisotropic conductance of the muscle fibers. The FHN equations add a non-linear reaction term to a transient diffusion equation in order to represent the ion current flows, which drive the depolarization and repolarization processes through the intra- and extracellular domains. The FHN model also includes an ODE to account for the recovery potential contribution responsible of the excitable media repolarization.

The proposed methodology is illustrated with numerical simulations both in academic simple geometries and in patient-specific cardiac ventricular. The latter have been reconstructed by using automatic three-dimensional medical image segmentation and mesh generation tools.

1 INTRODUCTION

Cardiovascular diseases (CVD) made up 29.2 percent of total global deaths according to a recent World Health Report [4]. It is estimated that by 2010, CVD will be the leading cause of death in industrialized countries. The major CVD include coronary (or ischaemic) heart disease (heart attack), cerebrovascular disease (stroke), hypertension (high blood pressure), rheumatic heart disease and heart failure. Damage to the heart tissues from CVD or from heart surgery can disrupt the natural electrical impulses of the heart and result in cardiac arrhythmia [1, 3].

Theoretical studies into the mechanisms of cardiac arrhythmias form a well-established area of electrophysiology but, despite decades of research, their causes are still poorly understood [24]. Experimental and clinical studies involving the in-vivo human heart are possible and often available in cardiac electrophysiology, but they are expensive and very limited. Therefore, well-defined mathematical and numerical modeling (computational models) of cellular electrophysiology and action potential propagation are becoming of great importance for understanding the developing and propagation mechanisms of arrhythmias and other pathologies. Nowadays, a challenge is to design tools for using such models in concrete medical applications, such as realistic simulations for prevention, diagnosis and therapy of cardiac diseases [5]. This is the main motivation for the work in progress that is presented in this paper.

From the early sixties, generic models of single-cell (microscopic level) have been created for a wide range of species and cardiac cell types (a detailed list is given in reference [22]). These models have achieved a high degree of detail in the description of cellular ionic currents and dynamics of several intracellular structures. They have been used to advance the understanding of processes influencing in specific patho-physiological responses, and have also been successful in describing cell properties. Despite all these advantages, it is impracticable to derive a whole heart (macroscopic level) by modeling every single cell that it contains [15]. The most obvious reason of this impossibility is the huge computing requirements, although the inaccuracy in determining both geometrical and physiological cardiac parameters represent nowadays a major problem to deal with real cases.

Since the mid-forties, several methods have been developed in order to simulate the electrical propagation of excitable media (at macroscopic or multicellular level) such as the cardiac tissue: reaction-diffusion systems, cellular automata, hybrid models [22]. Initially, they were used to reproduce excitation propagation in two-dimensional sheets of cardiac muscle. In the last years, several works have shown that these models can also be applied to describe three-dimensional phenomena [16, 20]. These models do not take into account microscopic cellular behaviour, which constitutes main limitations in their realism and applications.

During the past two decades, different modeling approaches have been developed for bridging in an efficient and realistic way the physical scales corresponding to different levels of anatomy (structural description) [6, 27]. This process is part of a general one

called integrative biological modeling, which is currently an active research topic that includes structural, functional and data integrations [15]. Currently, the most employed methods for bridging scales correspond to cellular automata and reaction-diffusion systems. The former are based on two components: discrete network of cells representing the spatial structure, and *a priori* definition of simple communication rules between cells in order to reproduce the propagation wave. The latter are based on conservation laws and use systems of partial and ordinary differential equations to describe the excitation and propagation process in cardiac tissue (excitable media). The present paper is based on this second line of action.

The paper introduces a new scheme to stabilize spurious effects due to non-linear terms, which eliminates non-physical numerical oscillations. Besides, a proper treatment of the non-linearities allows larger time steps in implicit schemes. Time discretization is handled either using a fully explicit Forward-Euler scheme or an implicit Crank-Nicholson scheme. Space discretization scheme is based on the Finite Element Method (FEM), particularly well suited for the involved complex cardiac geometries. An additional reason for using such a space discretization strategy is to apply FEM-bred consistent shock capturing techniques (SCT) to tame a major source of numerical instabilities: the steep electrical propagation front. The proposed SCT is inspired in computational fluid dynamics schemes.

The remaining of the text is organized as following. Section 2 gives a description of the model used for the simulations. Numerical schemes are explained in Section 3. Results are presented in Section 4. Finally, Section 5 closes the work with conclusions and suggestions for future research.

2 MODEL DESCRIPTION

2.1 Overview of Cardiac Electrophysiology

The origin of the electrical activity of the heart are the myocytes (cardiac cells), which form what is called an *excitable media* [2, 7]. In a normally functioning heart the electrical impulse starts in the sinoatrial node, located at the top of the right atrium (Figure 1). This node is the natural pacemaker of the heart, and consists of specialized cells which generate spontaneous and regular electrical action potentials. These action potentials spread throughout the right atria to the atrioventricular node and via the Bachmann bundle to the left atrium. The atrioventricular node delays the propagation, which is necessary for an appropriate and synchronized contraction of atria and ventricles. Thereafter the conductivity system of the ventricles, formed by the His bundle and the subendocardially located Purkinje fibers, is activated. Finally, the excitation passes to the ventricular myocardium, wherefrom it propagates to epicardial surface.

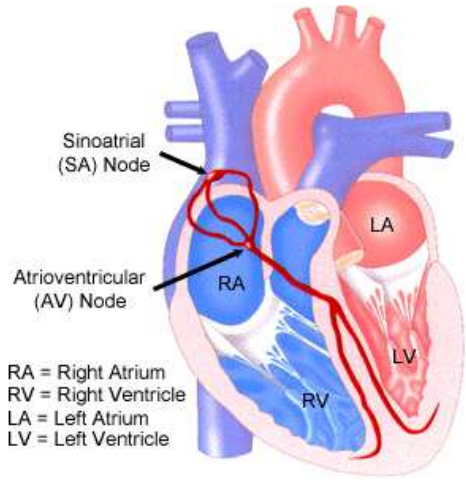

Figure 1: Heart Conduction System (taken from www.texasheartinstitute.org/HIC/Anatomy/).

2.2 Physical Model

Cardiac electrophysiology is modeled from both the macroscopic (cardiac tissue as a composite material) and the microscopic (cell-to-cell propagation) points of view. The global view can be condensed in a system of transient diffusion PDEs, which include terms that injects microscopic contributions in the macroscopic model. The canonical way of dealing with the macroscopic propagation of an action potential wave in the myocardial tissue is the *bidomain model*. Its main idea is to consider intra- and extracellular domains separated by a membrane, modeling their mean behavior. This allows taking into account the different conductivities of both media. There are several ways of treating the microscopic flow of ionic currents that drive the propagation process. In this paper (considered as a starting point for future research) we have chosen the FitzHugh-Nagumo model for leading this role. Both models are briefly explained below.

2.2.1 The Bidomain Model

The *Bidomain Model* treats the myocardial tissue as a continuum medium consisting of the intra- and the extracellular domains, which are separated by a membrane. A third domain, known as extramyocardial space, may be also defined and corresponds to any region outside of the heart [12]. Electrical propagation occurs along the membrane situated between the intra- and extracellular spaces. Solution of full bidomain equations is known to be important when modeling the efects of electric field stimulation on cardiac electrical responses [27].

The bidomain equations are derived by applying conservation of charge between the intra- and extracellular domains, which are characterized by conductivity tensors D_i and D_e, respectively. Between these two domains a current density I_m flows (Figure 2). The mathematical formulation of the bidomain model depicts the mutual dependency of in-

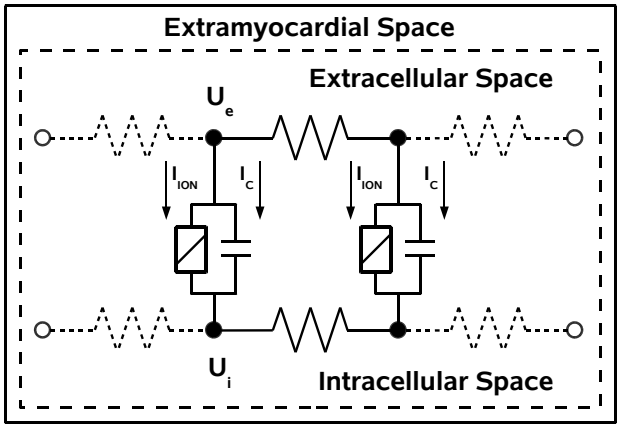

Figure 2: Schematic representation of one-dimensional bidomain model.

tracellular U_i, extracellular U_e, and transmembrane V_m potentials [6, 22]:

$$\nabla \cdot (D_i \nabla V_m) + \nabla \cdot (D_i \nabla U_e) = I_m \quad (1)$$

$$\nabla \cdot ((D_i + D_e) \nabla U_e) = -\nabla \cdot (D_i \nabla V_m) \quad (2)$$

$$V_m = U_i - U_e \quad (3)$$

The bidomain model is completely defined by equations (1,2). The transmembrane potential is the coupling variable when defining the microscopic contribution, as shown in the following section.

2.2.2 The FitzHugh-Nagumo Model

There are several methods [14, 18, 22] for modeling the current density I_m specified on equation (1). The *FitzHugh-Nagumo Model* represents the cellular response (excitability, threshold, depolarization, plateau, repolarization) to a stimulus in a compact and simple way. This model is a good tradeoff between complexity and computational efficiency, having been, for that reason, chosen in the present work. Its main disadvantage is the purely *ad-hoc* character of its derivation, not at all a consistent *bridging scale* model to connect micro and macroscopic scales. However, this model should be considered as the first step on the way of an accurate simulation of cardiac behaviour.

The FitzHugh-Nagumo model derives from the Hodgkin-Huxley equations [11]. The cellular electrical activity is controlled by transmembrane V_m and recovery W potentials [8] through the following equations:

$$I_{ion} = c_1 V_m (V_m - \alpha)(V_m - 1) + c_2 W \quad (4)$$

$$\frac{\partial W}{\partial t} = \varepsilon (V_m - \gamma W), \quad (5)$$

which leads to the definition of I_m as

$$I_m = S_v \left(I_c + I_{ion} + I_{st}\right) = S_v \left(C_m \frac{\partial V_m}{\partial t} + c_1 V_m (V_m - \alpha)(V_m - 1) + c_2 W + I_{st}\right) \tag{6}$$

where I_c, I_{ion} and I_{st} are the capacitive, ionic and stimulation currents, respectively. The parameters S_v and C_m correspond to membrane surface-to-volume ratio and membrane capacitance, respectively. The constants c_1, c_2, α, ε and γ are related with the duration and amplitude of action potential [16, 20].

2.3 Geometry

Electrical propagation is computed in three different geometries. First, a square of cardiac tissue is used for simulations (Figure 3, left). Although this is an academic geometry, it is useful for studying the behavior and dynamics of cardiac wave propagation. Later, simulation is performed on a geometry corresponding to a three-dimensional holed block of cardiac tissue (Figure 3, center). Finally, simulation is computed in left cardiac ventricle (Figure 3, right). This kind of geometry is more realistic, and it can be generated automatically from medical images by using segmentation techniques [19, 25].

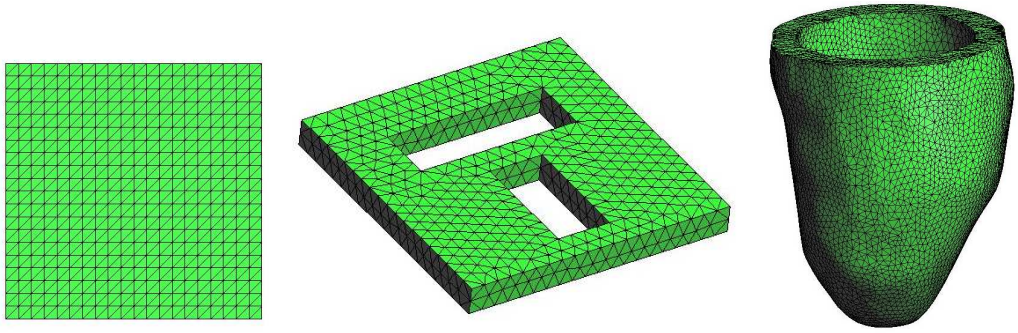

Figure 3: Geometries used for simulations of electrical propagation: a square (left), a 3D holed block of cardiac tissue (center), and the left cardiac ventricle (right).

2.4 Initial Conditions

The heart is polarized at the beginning of cardiac cycle. It means that intracellular, extracellular and transmembrane potentials correspond to resting state. Then, a good approximation for initial conditions can be done by using resting values of potentials for every point x that belongs to the heart:

$$\begin{aligned} V_m(x,0) &= V_{m0}(x) \\ U_e(x,0) &= U_{e0}(x) \end{aligned} \tag{7}$$

The resting state changes when the impulse originated in the sinoatrial node starts the depolarization process. The responsible for the transmission of this activation potential

to the left ventricle is the system formed by Purkinje fibers. This system of ventricular activation is included in the model through the stimulation current I_{st} of equation (6). Unfortunately, the orientation and position of such fibers is unknown. Then, any criterion has to be defined for the activation process. In the present work, a punctually excitation will be applied in the ventricular apex.

2.5 Boundary Conditions

Although the heart is not an isolated organ, we assume no electrical interaction with other parts of the body. This condition is reasonable for the sort of electrophysiology models addressed here [6, 16, 22]. For that reason, boundary conditions are set as

$$\begin{aligned} n \cdot (D_e \nabla U_e) &= 0 \\ n \cdot (D_i \nabla U_e) &= -n \cdot (D_i \nabla V_m)\,, \end{aligned} \tag{8}$$

which are the so called natural boundary conditions of the FEM-based formulation.

3 COMPUTATIONAL IMPLEMENTATION

Combining the macroscopic model equations (1,2,3) with those of the microscopic FHN (4,5,6) leads to the complete set of equations to be modeled:

$$\begin{aligned} S_v \left(C_m \frac{\partial V_m}{\partial t} + c_1 V_m (V_m - \alpha)(V_m - 1) \right) &- \nabla \cdot (D_i \nabla V_m) = \\ &= \nabla \cdot (D_i \nabla U_e) - S_v \left(c_2 W + I_{st} \right), \end{aligned} \tag{9}$$

$$\nabla \cdot \left((D_i + D_e) \nabla U_e \right) = -\nabla \cdot (D_i \nabla V_m)\,, \tag{10}$$

$$\frac{\partial W}{\partial t} = \varepsilon \left(V_m - \gamma W \right), \tag{11}$$

to be solved providing the proper boundary and initial conditions.

The FEM-based space-discretized weak form of the first two equations, combined with a finite differences based time discretization of the full set, leads to the following:

$$\left[c_T \frac{\boldsymbol{M}}{\Delta t} + \theta \boldsymbol{K_i} + \boldsymbol{I_{NL}^{imp}} \right] \boldsymbol{V_m}^{n+1} = \boldsymbol{f_m}^{n} \tag{12}$$

$$\boldsymbol{K_{tot}} \boldsymbol{U_e}^{n+1} = \boldsymbol{f_e}^{n} \tag{13}$$

$$\boldsymbol{W}^{n+1} = \boldsymbol{W}^{n} + \Delta t \varepsilon (\boldsymbol{V_m}^{n+1} + \gamma \boldsymbol{W}^{n}), \tag{14}$$

where bold face characters represent the nodal discretized variables, vectors (like $\boldsymbol{V_m}$ or $\boldsymbol{W}$) or matrices (like $\boldsymbol{K_{tot}}$ or $\boldsymbol{M}$). The right hand sides $\boldsymbol{f_m}^{n}$ and $\boldsymbol{f_e}^{n}$ include all the terms

evaluated at the previous time step and coming from the discretized equations. The factor $0 \leq \theta \leq 1$ is the trapezoidal rule parameter that discriminates between explicit ($\theta = 0$) or implicit ($0 < \theta \leq 1$) algorithms, notably $\theta = 0.5$ for second order Crank-Nicholson. $\boldsymbol{K_{tot}}$ represents the total diffusion matrix, which is computed with $D_{tot} = D_e + D_i$. The matrix $\boldsymbol{M}$ is the mass matrix, lumped using closed integration rules to make it diagonal and very convenient in explicit schemes or consistently (non-diagonal) computed for implicit schemes.

The non-linear term coming from the FitzHugh-Nagumo model $c_1 V_m (V_m - \alpha)(V_m - 1)$ deserves a special treatment, explained in the following section. Finally, shock capturing techniques are addressed.

3.1 Special scheme for Non-linear FitzHugh-Nagumo terms

Differential equation (9) presents a non-linear term, which can produce numerical instabilities. These can generally be removed by using small time steps, but sometimes this is computationally expensive. Then, it is convenient to design schemes with more robustness that can admit longer time steps. Next, a new scheme inspired in reference [9] is explained.

The basic idea is to combine different discrete linearizations of the diffusion-free model (6) in order to obtain a new scheme that improves numerical approximation for non-linear term. The proposed discrete linearizations DL_i are the following:

$$DL_1 = -c_1 a V_{m_{n+1}} + c_1(1+a)V_{m_n}^2 - c_1 V_{m_n}^3 \quad (15)$$

$$DL_2 = -c_1 a V_{m_n} + c_1(1+a)V_{m_n}^2 - c_1 V_{m_n}^2 V_{m_{n+1}} \quad (16)$$

$$DL_3 = -c_1 a V_{m_n} + c_1(1+a)V_{m_n} V_{m_{n+1}} - c_1 V_{m_n}^3 \quad (17)$$

where V_{m_n} and $V_{m_{n+1}}$ are the values for steps n and $n+1$, respectively.

If local truncation errors of equations (6,15,16,17) are combined in order to satisfy an specific equation, a more robust and better order method for non-linearities treatment can be constructed (see reference [21] for more details):

$$V_{m_{n+1}} = \frac{2 - c_1 a \Delta t + c_1 \Delta t V_{m_n}^2}{2 + c_1 a \Delta t - 2c_1(1+a)\Delta t V_{m_n} + 3c_1 \Delta t V_{m_n}^2} V_{m_n} \quad (18)$$

The new scheme is built by replacing equation (18) in the corresponding term of equation (12).

3.2 Shock capturing techniques

The choice of the finite element spaces where the approximated solutions are sought to conditionate the behavior of those solutions facing some special terms present in the equations. Particularly, non-linear terms are very likely to produce solutions with very strong gradients. The FEM spaces, spanned by compact support functions centered in the nodes, will then introduce spurious numerical oscillations localized around the strong

gradients, which are artifacts of non-physical character. Examples of these cases are the numerical oscillations around the shock waves in supersonic flows simulations. In order to damp them, a *consistent* numerical diffusion must be added. *Consistent* means that it cannot modify the physics, acting only where it is needed to damp the spurious errors.

This feature is also observed in electrophysiology. The action potential wave is a steep front that propagates through the cardiac tissue, followed by a smooth decaying stage and terminated by a sharp depolarization. We have adapted the Anisotropic Shock Capturing (ASC) technique proposed in works like [10, 17, 26].

Suppose a diffusion-reaction equation like that of V_m. Let us simplify it and re-write it as:

$$\frac{\partial V}{\partial t} - \nu \frac{\partial^2 V}{\partial x_k \partial x_k} + S(V) = 0,$$

where we have denoted $S(V)$ the non-linear term coming from the FitzHugh-Nagumo Model and ν as a generic diffusion coefficient. The Einstein summation convention on repeated indexes is used. According to the aforementioned method, a numerical shock capturing diffusion ν_{sc} is computed elementary, at the Gauss points level:

$$\nu_{sc} = \frac{1}{2} \alpha_{sc} h \frac{|R(V^h)|}{|\nabla V^h|}. \tag{19}$$

This numerical diffusion is properly added in the corresponding (discretized weak form) diffusion terms. The supraindexed V^h represents the projection of the continuous action potential on the discretized space. $R(V^h)$ is the space-time (discretized weak form) equation residual, and h is a characteristic length of the discretization element, typically the radius of the inscribed sphere (or circle in 2D). When there is no convection terms (as it is the case) $\alpha_{sc} = 0.7$, a constant coming from numerical analysis. Note that the numerical diffusion ν_{sc} is only present when the discrete equation residual rises.

4 RESULTS

The system defined by equations (12,13,14) is here solved by using both implicit and explicit algorithms. Simulations are also performed applying different combinations between the proposed shock capturing technique (SCT), by a certain number of non-linear iterations (NLI), and a special scheme for the non-linear treatment (SNLT). All the simulations were computed by using values of parameters taken from references [16, 20]. A time step of 0.1 ms was used for comparison reasons and because it is a value that falls below the critical time step coming from stability conditions of explicit schemes. A summary of the experiments carried out is specified in Table 1.

Results obtained by using the explicit method are shown in Figure 4. It can be observed that non-physical numerical oscillations (red and blue lines) only appear when standard algorithm is used. These oscillations are eliminated applying the SCT (green and magenta lines). The SCT diffusion depends on the discretized (space-time) residual of the equation,

Label	SCT	NLI	SNLT	Algorithm
01	No	0	No	X-I
02	Yes	0	No	X-I
03	No	10	No	X
04	Yes	10	No	X-I
05	Yes	10	Yes	I

Table 1: Summary of performed experiments. The first column corresponds to the number specified in labels of Figures 4 and 5. The second column indicates if shock captures technique (SCT) is used or not. The number of non-linear iterations (NLI) is shown in third column. The fourth column indicates if the scheme for non-linear treatment (SNLT) is applied or not. The last column denotes if the algorithm used is implicit (I) or explicit (X).

which must be computed as accurately as possible. We have observed that this fact is critical when considering the non-linear terms contribution to the residual, yielding to over diffusion. This is easily solved by some internal iterations done at each of the time steps (magenta line). In any case, it is worth to mention the advancing time step of explicit algorithms must fall below the causality limit. In the present problem, the critical time step has always been taken from the diffusivity limit.

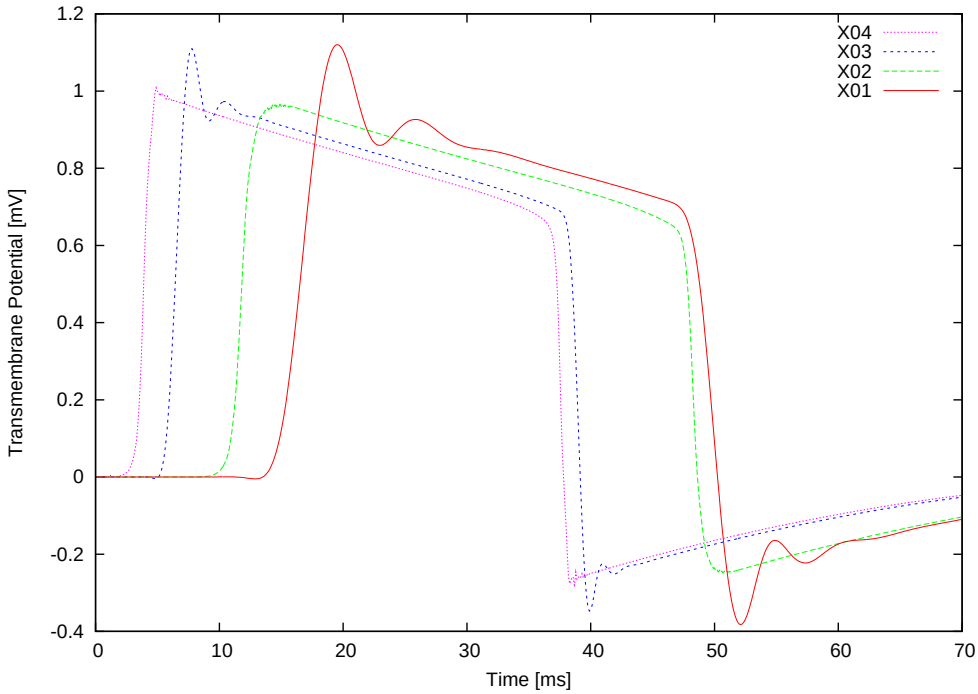

Figure 4: Numerical solutions obtained by using Explicit Method. Each line is the result of a simulation performed according to the numerical scheme specified in Table 1.

Results shown in Figure 5 correspond to those computed by using the implicit method. Just like in the results of the explicit algorithm, non-physical numerical oscillations (green

line) only appear when the standard algorithm is used. These oscillations are eliminated adding the SCT (blue, magenta and cyan lines). Again, the best results come when applying non-linear internal iterations (magenta and cyan lines). Due to the implicit character of the algorithm, the non-linear terms must be specially treated in order to damp the remnants of the spurious oscillations in the propagation front. This final correction is tamed by using SNLT (cyan line).

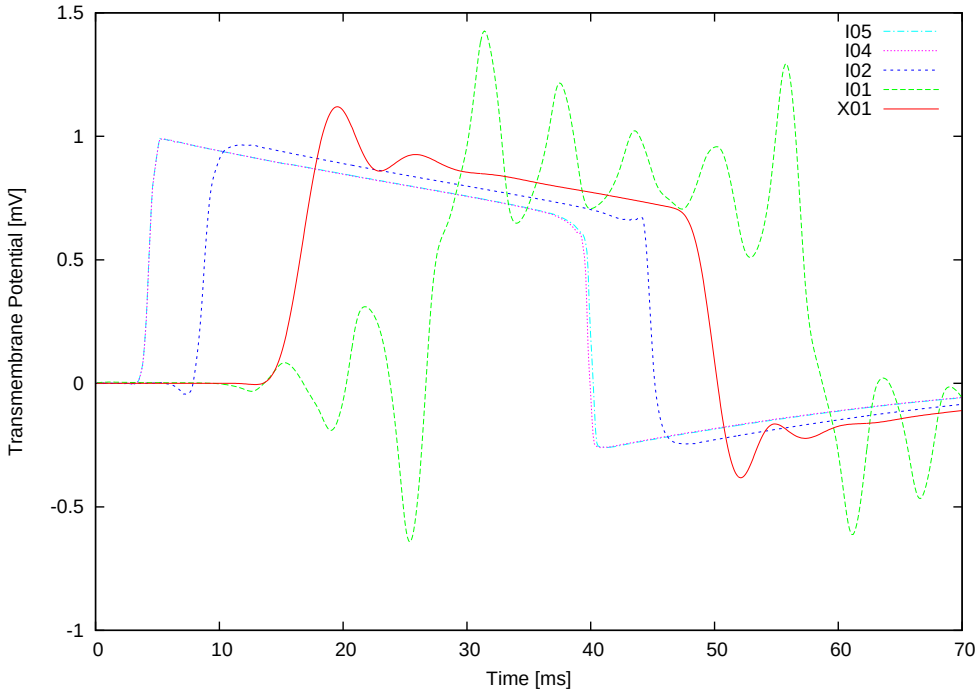

Figure 5: Solutions obtained by using Implicit Method (red line is only kept like reference). Numerical scheme used for computation of each curve is specified in Table 1.

Results shown in Figures 4 and 5 were obtained for a specific point of the square geometry indicates in Figure 3 (left). Temporal evolution of the electrical wave front corresponding to the holed block (Figure 3, center) is shown in Figure 6.

Results of simulation performed on a patient-specific ventricular geometry (Figure 3, right) are shown in Figure 7. It can be observed that three-dimensional cardiac electrical propagation is isotropic, which is not physiologically realistic. This problem can be corrected by using anisotropic diffusion tensors which depends on the cardiac fiber orientation. Future works will describe how this is implemented.

5 DISCUSSION AND CONCLUSIONS

The propagation of cardiac electrical activity was computed in three examples: a square, a holed block and a cardiac ventricular geometry by using a combination of FitzHugh-Nagumo and Bidomain models. The model equations were solved numerically

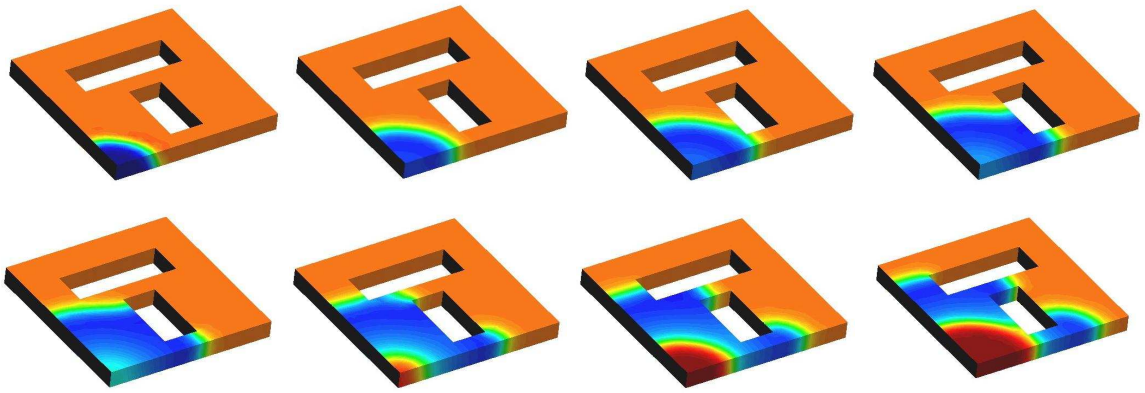

Figure 6: Three-dimensional electrical propagation in a holed block of cardiac tissue.

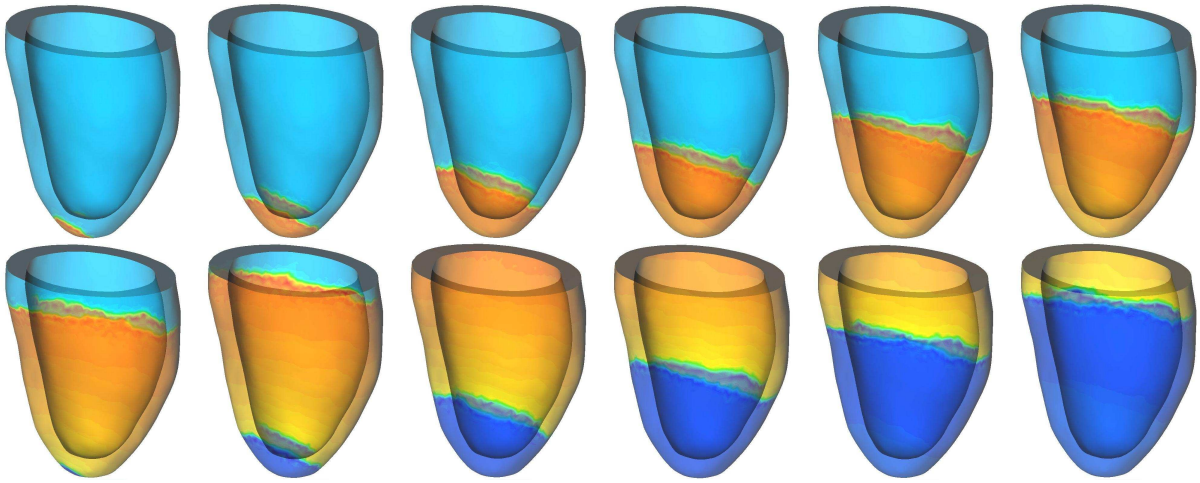

Figure 7: Three-dimensional cardiac electrical propagation in a patient-specific ventricular geometry.

by using FEM-based algorithms for the space discretization. Time was discretized using a finite differences scheme, allowing both implicit and explicit algorithms. Different numerical schemes were introduced in order to improve the behavior of non-linear terms.

These first results are promising and encourage the authors to face new research lines in order to improve in different aspects. The main points to attack are at what extent the physiological models used are realistic, how to improve the models by coupling mechanics and blood flood or how to include the indidual patients modeling parameters. Another important issues come from the pure computing side of the problem, like how to efficiently parallelize the schemes or how to deal with dynamic geometries.

Orientation of cardiac fibers was considered isotropic. This assumption can be used as a first approach, but it is far from being realistic. It means that an anisotropic orientation must be included, which could be done by mapping experimental measurements or by

creating a synthetic model according to literature [13, 23].

FitzHugh-Nagumo model approximately reproduces several features of the action potential. However, if we would like to study the relationship between a specific pathology and the observed electrical variations, a better ionic model would be necessary. A more detailed ionic model would also be necessary for a precise description of the electrical potential in function of information at microscopic level. Initial excitation has to be changed for taking into account Purkinje fibers. Unfortunately, there is not data available due to the technical difficulties inherent to the measure procedure. Although this fact conditionates any work that can be done, it must not refrain computational mechanics researchers from going ahead with their work to get the best possible simulation strategies and tools.

Results of the simulations should be compared with experimental measurements in order to adjust the parameters of each model. Such comparison is also necessary for patient-specific model characterization and validation.

REFERENCES

[1] Cardiovascular disease: www.healingwithnutrition.com/cdisease/cardiovascular/

[2] Cardiovascular Physiology Concepts: www.cvphysiology.com/

[3] Loyola University Health System: www.luhs.org/health/topics/cardiac/

[4] World Health Organization: www.who.int

[5] N. Ayache. *Computational Models for the Human Body*, Handbook of Numerical Analysis Vol XII, P.G. Ciarlet Editor, N. Ayache Guest Editor, Elsevier, 2004.

[6] M.E. Belik and T.P. Usyk and A.D. McCulloch. *Computational Methods for Cardiac Electrophysiology*, Computational Models for the Human Body, Handbook of Numerical Analysis Vol XII, P.G. Ciarlet Editor, N. Ayache Guest Editor, Elsevier, 129–187, 2004.

[7] R.M. Berne and M.N. Levy. *Fisiología* (Spanish Translation of 3 ° English Edition), Harcourt, Madrid, 2001.

[8] M. Boyett and A. Clough and J. Dekanski and A. Holden. *Modeling Cardiac Excitation and Excitability*, Computational Biology of the Heart, Ch 1, A. Panfilov and A. Holden Editors, John Wiley & Sons, 1–47, 1997.

[9] Z. Chen and A.B. Gumel and R.E. Mickens. *Nonstandard Discretizations of the Generalized Nagumo Reaction-Diffusion Equation*, Numer Methods Partial Differential, **19**: 363–379, 2003.

[10] R. Codina. *A discontinuity capturing crosswind dissipation for the finite element solution of the convection diffusion equation*, Comp Meth Appl Mech Eng, **110**: 325–342, 1993.

[11] R.A. FitzHugh. *Impulses and physiological states in theoretical models of nerve membrane*, Biophysical Journal, **1**: 445–466, 1961.

[12] A.F. Garny. *Advanced Computer Models of the Origin and Spread of Cardiac Propagation*, PhD thesis, University of Oxford, United Kingdom, 2004.

[13] P.A. Helm. *A Novel Technique for Quantifying Variability of Cardiac Anatomy: Application to the Dyssynchronous Failing Heart*, PhD thesis, Johns Hopkins University, Maryland, USA, 2005.

[14] P. Kohl and D. Noble and R.L. Winslow and P.J. Hunter. *Computational modeling of biological systems: tools and visions*, Phil Trans Royal Society London, **358**: 579–610, 2000.

[15] A.D. McCulloch and G. Huber. *Integrative biological modeling 'in silico'*, 'In Silico' Simulation of Biological Processes, Novartis Foundation Symposium 247, John Wiley & Sons, G. Bock and J.A. Goode Eds., 4–19, 2002.

[16] M. Murillo and X.C. Cai. *A fully implicit parallel algorithm for simulating the nonlinear electrical activity of the heart*, Numerical Linear Algebra with Applications, **11**: 261–277, 2004.

[17] P. Nithiarasu and O.C. Zienkiewicz and B.V.K. Satya Sai and K. Morgan and R. Codina and M. Vázquez. *Shock capturing viscosities for the general fluid mechanics algorithm*, International Journal of Numerical Methods in Fluids, **28**: 1325–1353, 1998.

[18] D. Noble. *The heart cell 'in silico': successes, failures and prospects*, 'In Silico' Simulation of Biological Processes, Novartis Foundation Symposium 247, John Wiley & Sons, G. Bock and J.A. Goode Eds., 182–194, 2002.

[19] S. Ordas and L. Boisrobert and M. Bossa and M. Laucelli and M. Huguet and S. Olmos and A.F. Frangi. *GRID enabled automatic construction of a two-chamber cardiac PDM from a large database of dynamic 3D shapes*, In R.M. Leahy and C. Roux Editors, IEEE International Symposium on Biomedical Imaging: From Nano to Macro, 416–419, 2004.

[20] R.C. Penland and D.M. Harrild and C.S. Henriquez. *Modeling impulse propagation and extracellular potential distributions in anisotropic cardiac tissue using a finite volume element discretization*, Computing and Visualization in Science, **4**: 215–226, 2002.

[21] A.M. Rosolen and M. Vázquez. BSC Technical Report, Barcelona, 2006. (*to appear*)

[22] F.B. Sachse. *Computational Cardiology: Modeling of Anatomy, Electrophysiology, and Mechanics*, Springer, Lecture Notes in Computer Science, Vol 2966, 2004.

[23] D.D. Streeter. *Gross morphology and fiber geometry of the heart*, in Handbook of Physiology: The Cardiovascular System, Berne Bethesda Ed, Vol I, American Physiology Society, pp 61-112, 1979.

[24] K.H. Ten Tusscher and D. Noble and P.J. Noble and A.V. Panfilov. *A model for human ventricular tissue*, Am J Physiol Heart Circ Physiol, **286**: 1573–1589, 2004.

[25] H.C. van Assen and M.G. Danilouchkine and A.F. Frangi and S. Ordas and J.J.M. Westenberg and J.H.C. Reiber and and B.P.F. Lelieveldt. *Spasm: a 3d-asm for segmentation of sparse and arbitrarily oriented cardiac mri data*, Medical Image Analysis, **10(2)**: 286–303, 2006.

[26] M. Vázquez. *Numerical modeling of compressible laminar and turbulent flow: the CBS algorithm*, PhD Thesis, Universitat Politècnica de Catalunya, Spain, 1999.

[27] R.L. Winslow and D.F. Scollan and A. Holmes and C.K. Yung and J. Zhang and M.S. Jafri. *Electrophysiological Modeling of Cardiac Ventricular Function: From Cell to Organ*, Ann Rev Biomed Eng, **2**: 119–155, 2000.